MICROCOPY RESOLUTION TEST CHART

NATIONAL BUREAU OF STANDARDS 1963 A

Outer Zone Electron Precipitation Produced
by a VLF Transmitter

A. L. VAMPOLA
Space Sciences Laboratory
Laboratory Operations
The Aerospace Corporation
El Segundo, CA 90245

and

C. D. ADAMS
Physics Department
University of Otago
Dunedin, New Zealand

1 March 1988

Prepared for

SPACE DIVISION
AIR FORCE SYSTEMS COMMAND
Los Angeles Air Force Base
P.O. Box 92960, Worldway Postal Center
Los Angeles, CA 90009-2960

DTIC
ELECTE
APR 0 4 1988
S
D
H

This report was submitted by The Aerospace Corporation, El Segundo, CA 90245, under Contract No. F04701-85-C-0086-P00016 with the Space Division, P.O. Box 92960, Worldway Postal Center, Los Angeles, CA 90009-2960. It was reviewed and approved for The Aerospace Corporation by H. R. Rugge, Director, Space Sciences Laboratory.
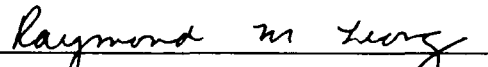
Lt Clarence V. Wilcox/CLTPC was the project officer for the Mission-Oriented Investigation and Experimentation (MOIE) Program.

This report has been reviewed by the Public Affairs Office (PAS) and is releasable to the National Technical Information Service (NTIS). At NTIS, it will be available to the general public, including foreign nationals.

This technical report has been reviewed and is approved for publication. Publication of this report does not constitute Air Force approval of the report's findings or conclusions. It is published only for the exchange and stimulation of ideas.

CLARENCE V. WILCOX, Lt, USAF
MOIE Project Officer
SD/CLTPC

RAYMOND M. LEONG, Major, USAF
Deputy Director, AFSTC West Coast Office
AFSTC/WCO OL-AB

8a. NAME OF FUNDING / SPONSORING ORGANIZATION	8b. OFFICE SYMBOL *(If applicable)*	9 PROCUREMENT INSTRUMENT IDENTIFICATION NUMBER			
		F04701-85-C-0086-P00016			
8c. ADDRESS *(City, State, and ZIP Code)*		10 SOURCE OF FUNDING NUMBERS			
		PROGRAM ELEMENT NO.	PROJECT NO.	TASK NO.	WORK UNIT ACCESSION NO.

11 TITLE *(Include Security Classification)*
Outer Zone Electron Precipitation Produced by a VLF Transmitter

12 PERSONAL AUTHOR(S)
Vampola, Alfred L.; and Adams, C. D., University of Otago

13a. TYPE OF REPORT	13b TIME COVERED FROM _____ TO _____	14. DATE OF REPORT *(Year, Month, Day)* 1988, March 1	15 PAGE COUNT 31

16 SUPPLEMENTARY NOTATION

17	COSATI CODES		18 SUBJECT TERMS *(Continue on reverse if necessary and identify by block number)*
FIELD	GROUP	SUB-GROUP	Electron Precipitation Van Allen Belts
			Magnetospheric Electrons Wave-Particle Interaction

PREFACE

1

CONTENTS

FIGURES

INTRODUCTION

The precipitation of magnetospheric electrons by gyroresonant interactions with electromagnetic waves from ground-based VLF transmitters has been a topic of growing interest for almost a decade. Vampola [1977a] presented observations of L-dependent precipitating energetic electrons ($E_e > 100$ keV) in the slot region of the magnetosphere which were correlated in longitude with the location of powerful ground-based VLF transmitters. In an L-dependent precipitation event, the higher energy electrons precipitate at lower L in an energy *vs* L relationship that can be shown to be consistent with a single resonant wave frequency. Vampola and Kuck [1978] used observations of inner-zone electrons in the drift loss cone with a trace-back technique to locate the actual transmitters which were causing the precipitation. Koons et al [1981] used structures in the inner-zone drift loss cone electron distributions and synoptic VLF data to correlate electron precipitation events with specific transmission sequences from the VLF transmitters UMS and NWC. Imhof et al [1983] correlated observations of precipitating electrons in the bounce loss cone of the outer edge of the inner zone with transmitting patterns from a ground-based VLF transmitter. Vampola [1983] used satellite observations of the depletion of electron fluxes transported across the slot region during a magnetic storm to determine the lifetime of inner-zone electrons against precipitation by VLF transmissions in order to determine the relative importance of VLF transmissions on the morphology of magnetospheric electrons. He concluded that the location and shape of the outer edge of the inner zone are controlled by ground-based VLF transmissions. Vampola [1987] used high-resolution pitch angle measurements of precipitating electrons in the slot region to determine the precipitation pattern around a VLF transmitter and made resonance calculations which indicated the interaction region for slot precipitation was well away from the equator.

While it is now generally accepted that man-made waves are instrumental in precipitating electrons at the outer edge of the inner zone, there has been much less acceptance of ground-based VLF transmitters being a significant factor in the precipitation of electrons in the slot region. Precipitation of electrons in the outer zone has not been associated previously with these ground-based VLF transmitters.

In surveys made by one of us (ALV) of large magnetospheric electron data bases obtained by a number of electron spectrometers flown on various satellites, a recurrent observation has been that electron precipitation occurs in "events" rather than in a slow diffusion process, especially in the slot region. Vampola and Gorney [1983] made a statistical study of energy deposition in the middle atmosphere by precipitating electrons and observed that for even as high as L=4 the hemispheric pattern of precipitation was that which would occur if electron scattering from stable drift orbits into the loss cone were primarily large angle scattering rather than a slow pitch angle diffusion. While it is known that non-resonant mechanisms precipitate electrons at times (e.g., electrostatic wave structures at the outer edge of the outer zone [Koons et al, 1972]), it is appropriate to question whether VLF transmitters are also instrumental in precipitating electrons in the outer zone. In this paper, we will show that VLF transmitters may, in fact, precipitate large numbers of electrons in the outer zone.

OBSERVATIONS

The data presented in this study were obtained on 28 July 1976 by a magnetic-focusing electron spectrometer on the USAF Space Test Program satellite S3-3 while the satellite was below the stable trapping region of the magnetosphere. That is, any electrons mirroring at or below the altitude of the satellite had had their pitch-angles lowered at some location during the time they drifted from approximately 30° east longitude (EL) to the location of the satellite at approximately 120° EL. West of 30o EL, the mirror altitudes would have been at or below 100 km, the nominal atmospheric absorption altitude. The spectrometer consisted of two separate analyzing chambers, one covering the energy range 12 keV to 162 keV in five differential energy channels and another covering the range 235 keV to 1630 keV in seven differential energy channels. The above energies refer to the centroid of the energy response for a "flat" (energy-independent) spectrum. The lower energy unit had a collimator with a 2°x5o half-angle response, the other had a 5ox5o half-angle collimator. Geometric-energy factors for the lower energy chamber were several orders of magnitude smaller than those of the higher energy chamber. The direction of scan (using the spin-stabilized spacecraft as a scanning platform) was across the 2° direction (in the plane of the instrument). The combination of spin rate, nominally 3 RPM, and read-out of accumulators, 16 times per second, provided pitch-angle measurements at about 1.1° intervals. For this study, data from the 108, 162, 235, 433, 654, and 880 keV channels only are used. The data from the 12, 33, and 70 keV channels were not used because the 70 keV detector was noisy and electrons of 12 and 33 keV may be present on the drift shell due to acceleration of ionospheric electrons up field lines by electrostatic potentials.

The event which is utilized in this study was characterized by precipitation peaks in the inner zone, the slot, and the outer zone. Events of this type are frequently seen whenever the satellite is in the drift loss cone of the longitudes associated with the transmitter UMS. In this study, 7% of the orbits examined had such combinations of slot and outer zone precipitation structures. Since many of the orbits examined did not include measurements in the drift loss cone, the actual incidence of such precipitations is higher. The specific event selected for analysis in this study was selected on the basis of: a) there being a statistically significant intensity in all three precipitation peaks in a single channel (required for determining the longitude of

9

origin); b) the observation of flux in two or more channels for each of the peaks (needed for a drift-rate analysis comparison with the transmission schedule of the transmitter); and c) the availability of the transmission schedule of the suspected transmitter for the time of the precipitation.

The precipitation event selected included measurable flux in channels up to the 880 keV channel, but the 235 keV channel had much higher counts due to the facts that the flux intensity decreased sharply with energy above 235 keV and that the lower energy chamber had geometric-energy factors much smaller than the higher energy chamber. Since accurate pitch angle determinations are required for the type of analysis which is used here, the 235 keV channel has been selected for primary presentation and analysis. The other channels are used to establish that precipitation features discussed here were L-dependent precipitation events and, because drift rates are strongly dependent on electron energy, for detailed comparison with the transmitting sequences of the presumed transmitter. In these events, the 235 keV channel typically had count-rates one to two orders of magnitude greater than any of the other channels. The absolute upper and lower limits of response of that channel are 320 keV and 158 keV, respectively, with 20% of the response being above 265 keV and 20% being below 200 keV, both figures referring to a "flat" spectrum. The geometric-energy factor for the 235 keV channel for a "flat" spectrum is 6.54 cm^2-ster-keV.

The counts/0.0625 sec from the 108 keV through 654 keV channels, converted to flux units using the "flat" spectrum geometric-energy factors, are shown in Fig. 1. A table at the bottom of the figure lists the geographic and geomagnetic coordinates of the satellite during the time the data were being obtained. The data have not been corrected for background effects. The dashed lines in the figure are the fluxes measured at the same L values at higher altitudes (between 3600 km and 7000 km, the higher value at higher L) in the opposite hemisphere and are included for comparative purposes.

Note that the data of Fig. 1 cover inner zone, slot and outer zone regions, all in the drift loss cone. Any electrons observed are only quasi-trapped, have been scattered down the field line somewhere between 30° EL and their present longitude, and will be lost into the atmosphere prior to or near the South Atlantic Anomaly. The numbers 3 through 5 in the 235 keV panel refer to the locations at which data were obtained for presentation in Figs. 3 through 5.
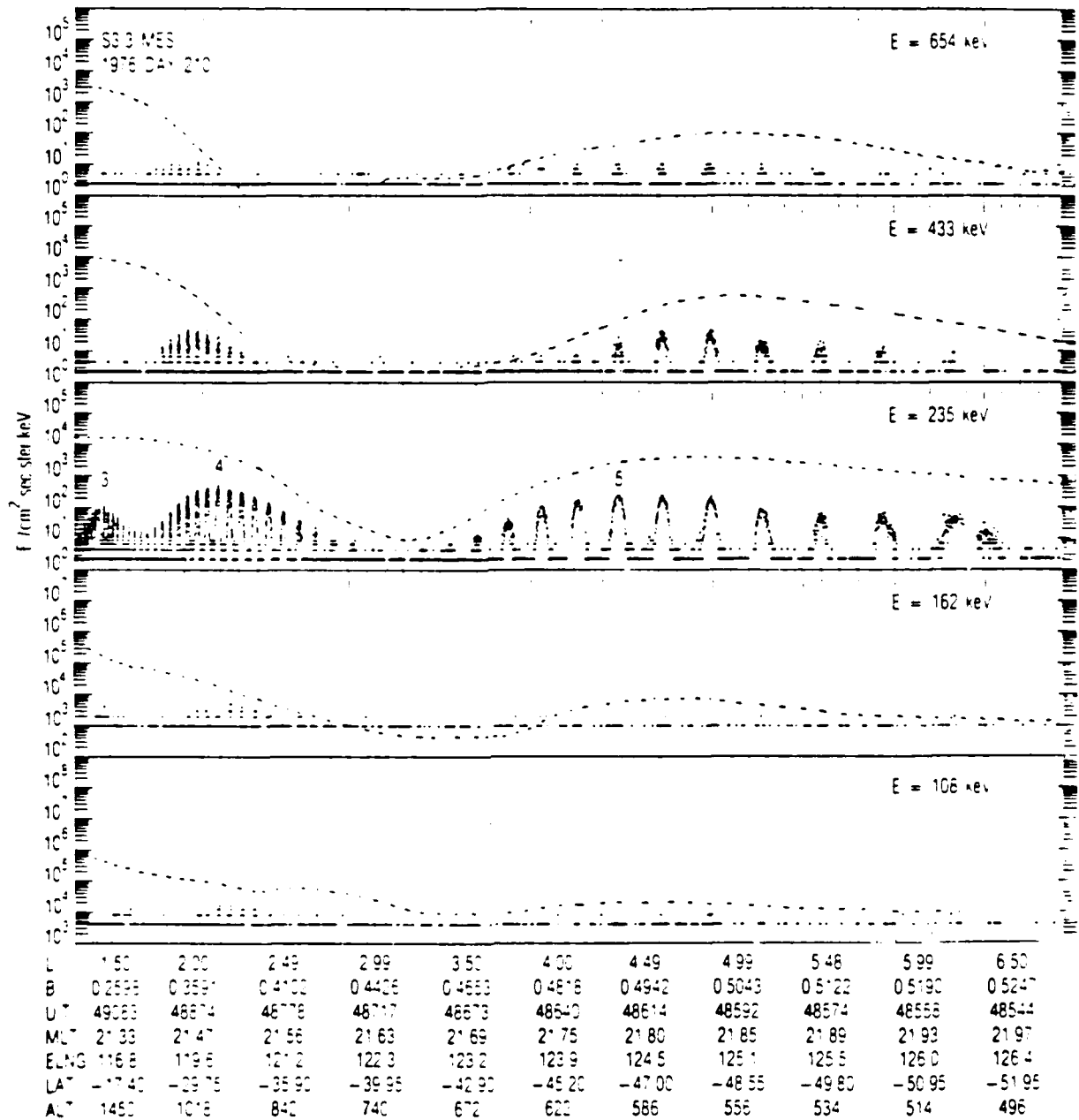
Figure 1. Electron fluxes from the S3-3 108 through 654 KeV channels obtained on 28 July 1976 while the satellite was below the stable trapping region of the magnetosphere. All electrons observed during this pass will be lost into the atmosphere before completing one drift orbit. Any electrons observed during this pass must have entered the drift loss cone east of about 30° east longitude. The dashed lines show stably trapped fluxes measured in the opposite hemisphere at altitudes between 3600 km (L=1.5) and 7000 km (L=7.0). The numbers 3-5 refer to the regions of data plotted in Figs. 3-5.

Figure 2 is a plot of the location in L of the peak precipitation observed in the inner zone in the 108, 162, 235, and 433 keV channels and in the slot at 108, 162, 235, 433, and 654 keV plotted at their nominal energies. The bars indicate the total energy span of each channel. The solid line is a calculation of the nominal equatorial resonant energy *vs* L for a wave of frequency 17.1 kHz (the UMS frequency) with a wave-normal angle of $60°$, a base density of $9200/cm^3$, and using a simple exponential decrease of electron density with altitude in a dipole field. The wave-normal angle was selected on the basis of a previous ray-tracing analysis in the inner zone for UMS [Koons et al, 1981]. The base density was selected as being the best fit to the ray-tracing analysis for the 235 keV channel data which is presented later in the Resonance Calculations section. There is no question that both the inner-zone and slot precipitation are L-dependent. The fit to the inner-zone precipitation peaks is not exact because a relatively crude resonance calculation was performed for Fig. 2 and, for reasons which will become clear later in the discussion, the energy of the particles detected by a given channel may not be well represented by using the centroid of response of that channel.

The first peak, labeled "3" in Fig. 1, is an L-dependent precipitation of the type analyzed in detail by Koons et al [1981]. Sufficient flux for L-determination was observed in the 108, 162, 235 and 433 keV channels, but due to the small geometric-energy factors of the lower channels only the 235 keV channel had a sufficient count-rate for pitch-angle determination with accuracy of the type required for use in a traceback-to-longitude-of-origin technique [Luhmann and Vampola, 1977]. Analysis of a large number of similar events by Vampola and Kuck [1978] indicated that inner-zone precipitation with energies in excess of 400 keV is rare, so it is probably not significant that few electrons were observed at energies above the 235 keV channel.

The traceback-to-longitude-of-origin technique is applicable to particles observed within the drift loss cone under the assumption that the particle pitch angle distribution was produced by interaction with the atmosphere at the longitude of precipitation and has not been substantially modified during the time the particles have drifted from their longitude of precipitation to the longitude of observation. The procedure requires transforming the local pitch angle to equatorial pitch angle and then matching the equatorial pitch angle cutoff to the equatorial atmospheric loss cone angle at some previous longitude, with the requirement that no intervening longitude has an atmospheric loss cone angle that is larger.
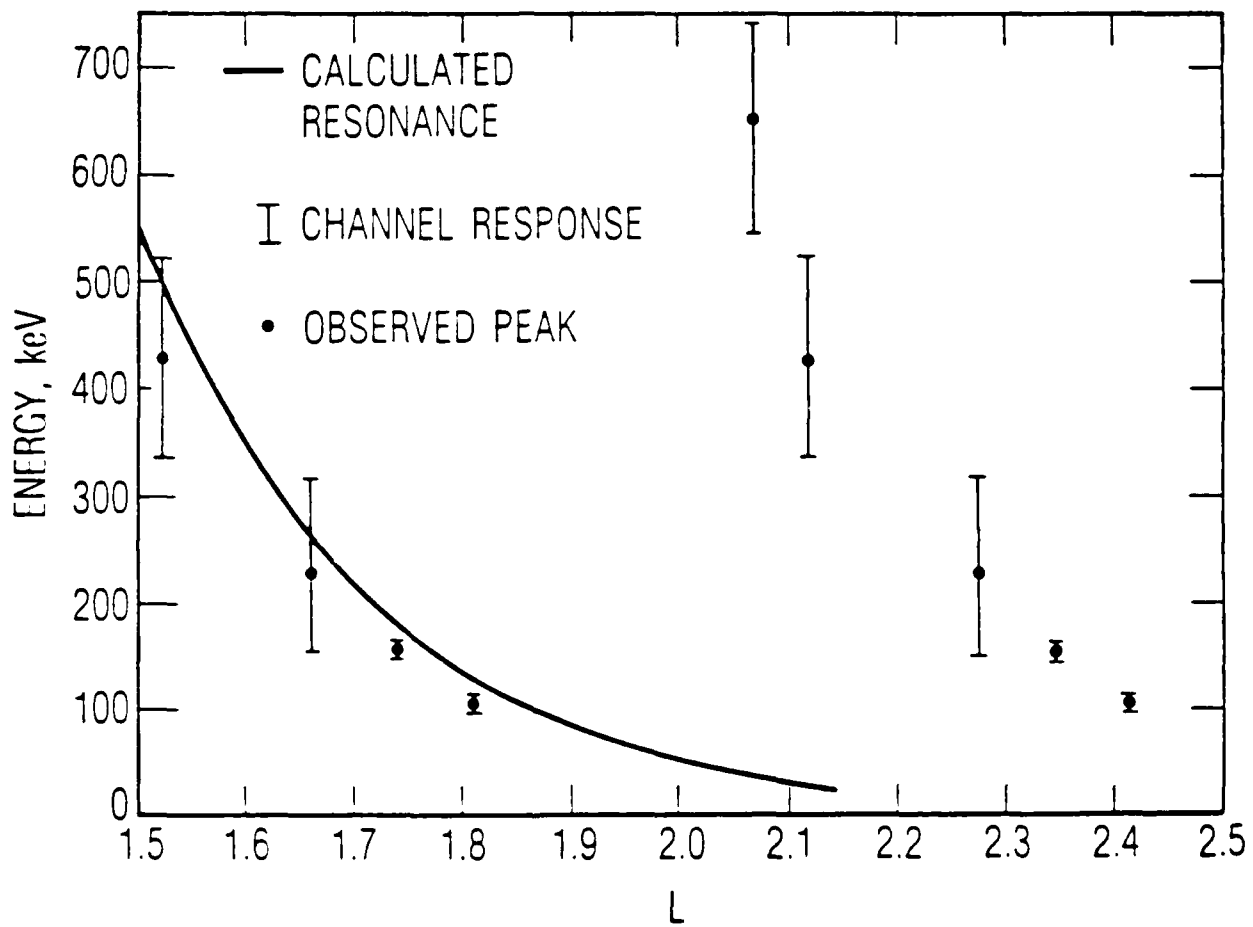
Figure 2. Calculated gyroresonant energy at the equator for a frequency of 17.1 kHz, a wave normal angle of 60°, and a base density of 9200/cm³. The dots are the inner zone precipitation peaks from the 108, 162, 235, and 433 keV channels and the slot precipitation peaks at 108, 162, 235, 433, and 654 keV plotted at their nominal energy. The bars indicate the total energy span of the channels.

Figure 3 presents the raw counts for one-half spin period of the satellite, normalized to the 85°-95° pitch angle average, plotted as a function of pitch angle for the data of peak 3 in Fig. 1. The L-value of this data, 1.66, is similar to those of the events reported by Vampola and Kuck [1978], Koons et al [1981], and by Imhof et al [1981] in which electrons in this energy range were being precipitated in the inner zone by VLF transmitters. The smaller intensity in this peak compared to peaks 4 and 5 is probably a matter of instrumental response, for reasons to be discussed later, and should not be taken as an indication that fewer electrons were precipitated in the inner zone. The dashed lines show the response of the instrument to a distribution in which the flux is zero within the local atmospheric loss cone and isotropic beyond it. The observed particle pitch angle distribution is much narrower than the local loss cone, indicating that the pitch angle distribution is not determined by local conditions but rather by scattering and atmospheric cutoff conditions at some previous longitude(s). The solid lines represent the instrument response to a distribution defined by isotropic precipitation at 45° EL, the western end of the UMS precipitation region [Koons et al, 1981]. The data are fit quite well by the assumption of a 45° EL origin. For a better fit to the slope of the pitch angle distribution, one would have to take into account the entire longitudinal precipitation pattern that is contributing to the data points, as was done in Vampola [1987]. The magnetic field model used for tracing purposes for this and the other peaks was the DGRF 1975 [IAGA, 1981], Epoch 1976, internal field model. No external field model was used. It can be concluded from the L-dependent nature of the precipitation, the fit of the L vs Energy dependency to the resonance calculation, and from the longitude of its origin that the flux in peak 3 was undoubtedly precipitated by the ground-based VLF transmitter UMS. The L-value of UMS varies from 1.73 to 1.77, depending on whether 44° EL or 56° EL and whether 0 or 100 km altitude is used for the determination. Calculations presented in the Resonance Calculations section were performed with the UMS frequency, 17.1 kHz, and location, 44° EL, 46.2° N [Watt, 1967].

Since the particles trace back to the western end of the UMS precipitation region, it appears that the particles may be the tail end of a longitudinal distribution due to a discrete transmission period. When the transmitter turns off, precipitation stops and the entire longitudinal pattern of precipitation drifts eastward, with different drift rates for different energies and L-shells. (The drift rate is relatively insensitive to pitch angle for the small variations in pitch angle of concern here.) We shall address this topic again in the Analysis section.
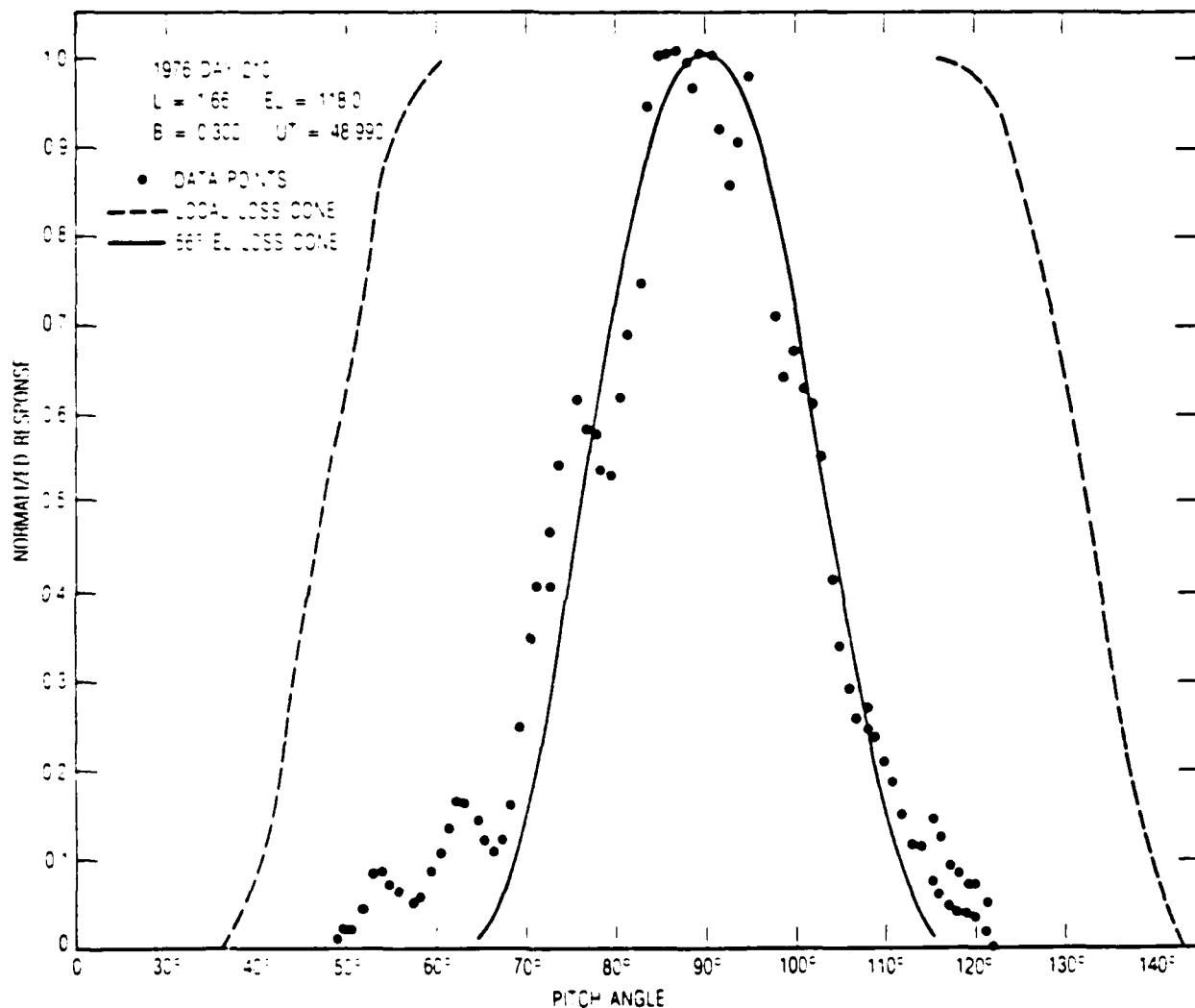
14

Figure 3. Pitch angle distribution of electrons in the 235 KeV channel observed in the L=1.66 drift shell compared with the local bounce loss cone (dashed lines) and the 100 km atmospheric loss cone at 45° east longitude (solid lines). The pitch-angle distributions match the 100 km atmospheric loss cone at the westernmost longitude of UMS precipitation. See text for details.

15

Figure 4 is similar to Fig. 3 but is slot data at a higher L-value than the inner-zone precipitation. The L-value is similar to that of the observations of Imhof et al [1983], but the energy is significantly higher. The observations of Imhof et al [1983] were at quite low energy and were the low energy extension (to higher L) of the inner-zone equatorial region electron precipitation by ground-based VLF transmitters (Vampola and Kuck [1978]). The peak of Fig. 4 was again an L-dependent peak as can be seen from Fig. 2, with strong fluxes (400 counts/sec) in the 235 keV channel, significant fluxes in the 433 keV channel, and traces of flux in the 108, 162, 654 and 880 keV channels. The dashed lines are again as defined in Fig. 3, but in Fig. 4 the solid lines represent the atmospheric loss cone at 56°, the eastern end of the UMS precipitation region. These match the data points, giving an unambiguous fit to the eastern end of the UMS precipitation region. Since the eastern end of the precipitation region has the smallest equatorial pitch angle cutoff, the simple comparison with pitch angle cutoffs being made here should always trace back to the easternmost longitude of the precipitation region that is currently represented in the drifting particles at the longitude of the satellite. Figures 3 and 4 indicate that a single transmitter, UMS, was probably precipitating electrons simultaneously on both an inner-zone field line and a slot field line. We will show later, using drift-rate analyses and the operating times of UMS, that this was indeed the case.

Figure 5 presents the L=4.48 data (peak 5 of Fig. 1) in a format similar to Fig. 3. For this event, flux was observable in the 235, 433 and 654 keV channels. These particles were precipitated east of 30° EL within the previous 18 minutes (the time for electrons with this energy, pitch-angle, and L-shell to drift from 30° EL, the westernmost location on this drift shell which can be observed by the satellite at this altitude and longitude). Due to the broad region over which the 235 keV channel is detecting electrons, it is difficult to assign a single L-value for the peak. The match between the solid lines and the data points in Fig. 5 again indicates that the electrons trace back to the eastern end of the UMS precipitation region and were precipitated in the vicinity of UMS. For both the L=2.28 and L=4.48 precipitation events, the trace-back is accurate to within several degrees of longitude of the eastern end of the UMS precipitation region. Two degrees in pitch angle are equivalent to about one degree in longitude around 56° EL for this geometry. The fact that this pitch angle distribution maps back to the location of UMS at a time when UMS was precipitating electrons from the inner zone and from the slot is indicative of these outer zone electrons being precipitated by UMS even though there is no obvious L-dependency.

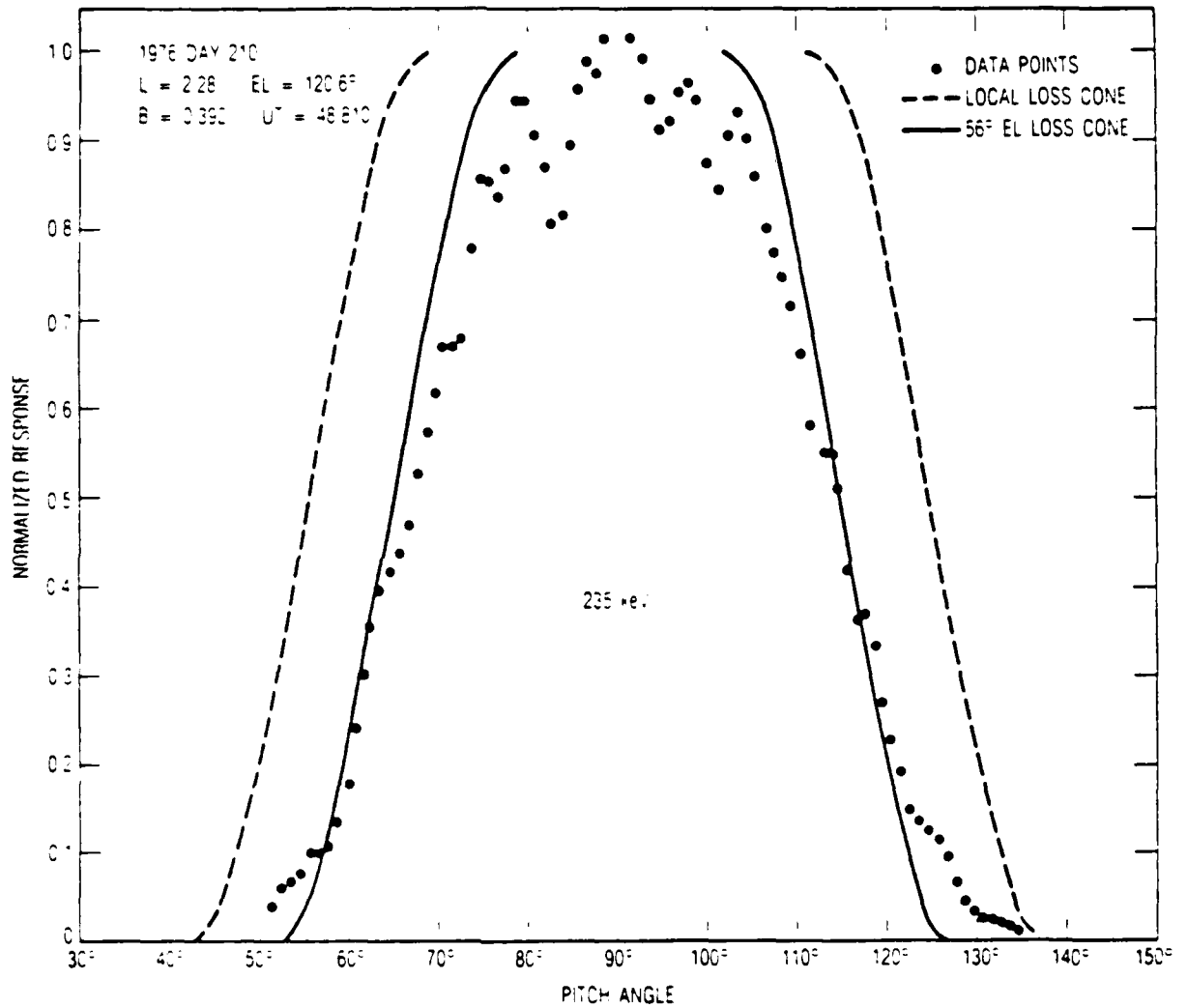Figure 4. Similar to Fig. 3, except that the electrons are in the L=2.28 drift shell and the solid lines represent the atmospheric loss cone at 56°. The fit to the atmospheric loss cone at the easternmost longitude of UMS precipitation (56°) is unambiguous.
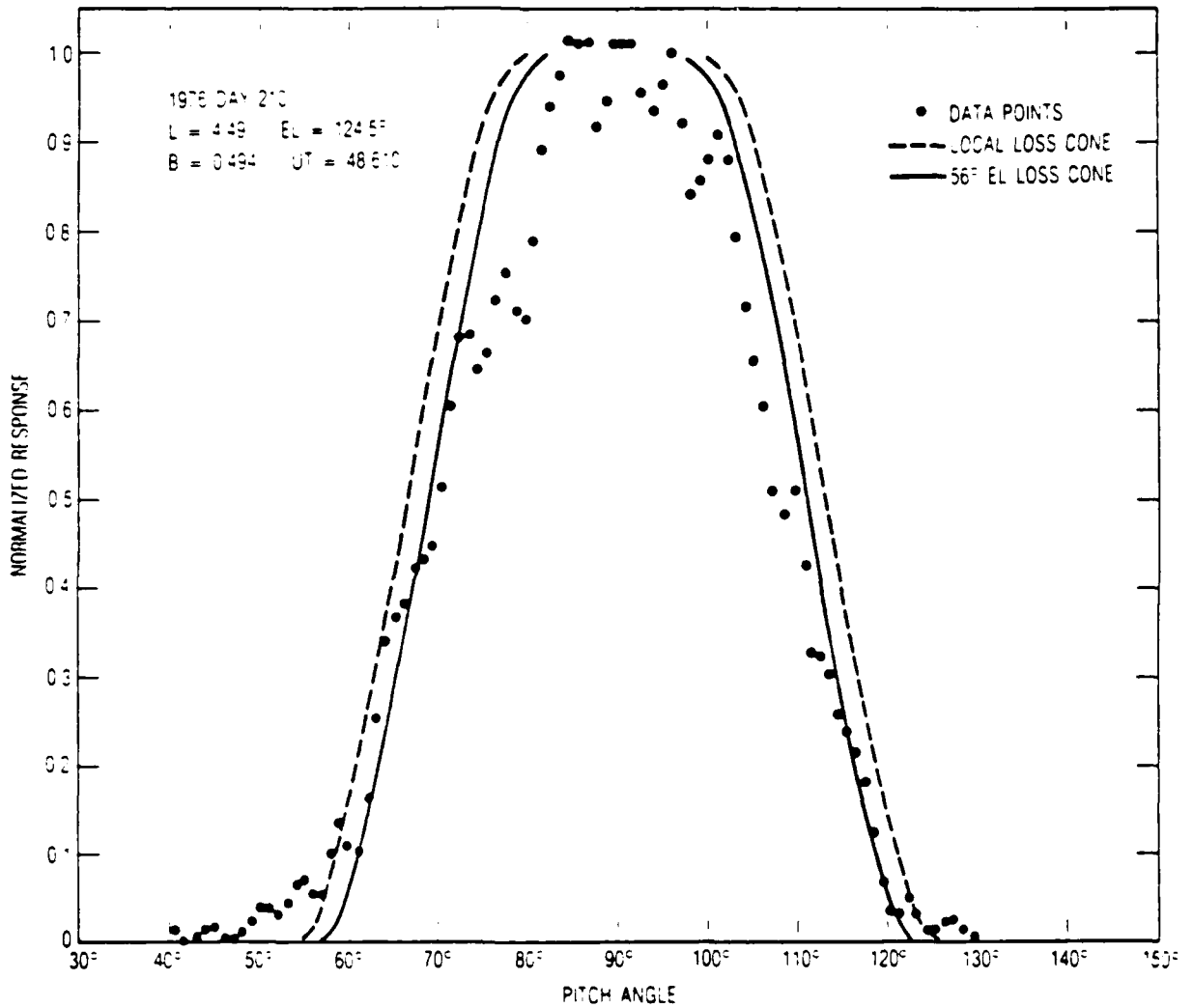
17

Figure 5. Similar to Figs. 3 and 4, but for the L=4.48 drift shell. Again, the data fit the atmospheric loss cone at the longitude of UMS.

18

ANALYSIS

Because of the highly surprising nature of the conclusion, above, that UMS was precipitating electrons from the outer zone, additional supportive evidence is necessary, even though the direct evidence is strong. Direct comparison of the transmitting schedule of UMS with the particle observations would be most helpful. If UMS were not operating, or if its operating schedule were not consistent with the particle observations, another explanation would have to be sought for the precipitations. Fortunately, the transmission sequence of UMS at the appropriate time is available for comparison with the drift rates of the electrons. One can calculate the drift rate for electrons of various energies on the various L-shells using the relationship [Schulz and Lanzerotti, 1974]:

$$2\pi/\Omega_2 = -(3L/2\pi\gamma)(\gamma^2-1)(c/a)^2(m_e/qB_o)D(y)/T(y)$$

where Ω_2 is the drift frequency, γ is the relativistic mass ratio of the electron, c is the velocity of light, a is the earth radius, L is in units of earth-radius, m_e is the mass of the electron, B_o is the value of the earth's magnetic field at the surface of the earth at the equator, q is the charge on the electron, y is $\sin\alpha$ where α is the equatorial pitch angle, and $D(y)$ and $T(y)$ are given by:

$$D(y) = {}^1/_{12}\{5.5208-.4381y-.6397(y \ln y + y^{1/2})\}$$

$$T(y) = 1.3802-.31985(y+y^{1/2})$$

By making use of the fact that electrons with various energies on a given L-shell drift with different rates, the data from each energy channel become a separate test of the validity of the assignment of UMS as the cause of the precipitation. Each operational period of UMS, precipitating all energies at the same time at the same longitudes, produces a series of longitudinally-drifting electron bunches characterized by a finite longitudinal length (determined by the length of time the transmitter is radiating and the longitudinal width of the interacting region) drifting with a rate that is energy dependent. At a given later time, different energies will be found at different longitudes,

with the higher energy electrons being farther east since they drift at a faster rate.

For the comparison with the UMS transmission schedule, data were extracted by Rayspan analysis from synoptic VLF recordings made at the time the satellite data were obtained. The receiver consisted of a vertical loop antenna of 100 square meters area with the plane of the loop oriented at 70° east of north, feeding a preamplifier covering the frequency range from 0.5 to 30 kHz. The preamplifier output was telemetered 10 km to the University of Otago campus by UHF link for analog recording on magnetic tape. Timing information accurate to a few milliseconds was provided by NASA-36 timecode recorded on a separate track.

In order to ascertain when UMS was transmitting, dynamic spectra from this tape in the range from 10-20 kHz were recorded on film using a modernized Rayspan real-time spectrum analyzer. This gave a detection limit for signals arriving from the direction of UMS of about 60 microvolts per meter while the UMS transmission was determined to have a signal strength of about 200 microvolts per meter. This indicates a radiated power level of several hundred kW based on sub-ionospheric propagation calculations following Watt [1967]. This power level is in agreement with published figures (315 kW, Watt [1967]) for UMS.

Using UMS transmission times from the Rayspan analysis and assuming that all energies of electrons are precipitated by UMS at all L-values, Fig. 6 diagrams the electron energies, as a function of L, that should be observable by the S3-3 as it crosses the various L-shells in the pass plotted in Fig. 1. The first transmission, which ended at 12:59:07 UT, is diagramed with both a 56° and a 45° cutoff, since the data of Fig. 3 indicate the inner-zone particles were precipitated near 45°. Electrons precipitated by the first transmission with energies above those given by the 45° line would have already drifted past the longitude of the satellite by the time the satellite arrived. Similarly, electrons precipitated at 56° with energies above the line marked 56° would also have drifted past the longitude of the satellite. For the second transmission, which began at 13:16:09 UT, electrons with energies below the line marked 56° would not yet have arrived at the longitude of the satellite. The vertical dashed lines marked 3, 4, and 5 indicate the L-values of the data of Figs. 3-5.

We will now compare the predictions of observable electron energies as a function of L in Fig. 6 with the actual observations. Figure 6 predicts that electrons with energies between about 120 keV and 155 keV precipitated at 56° EL by the first

20
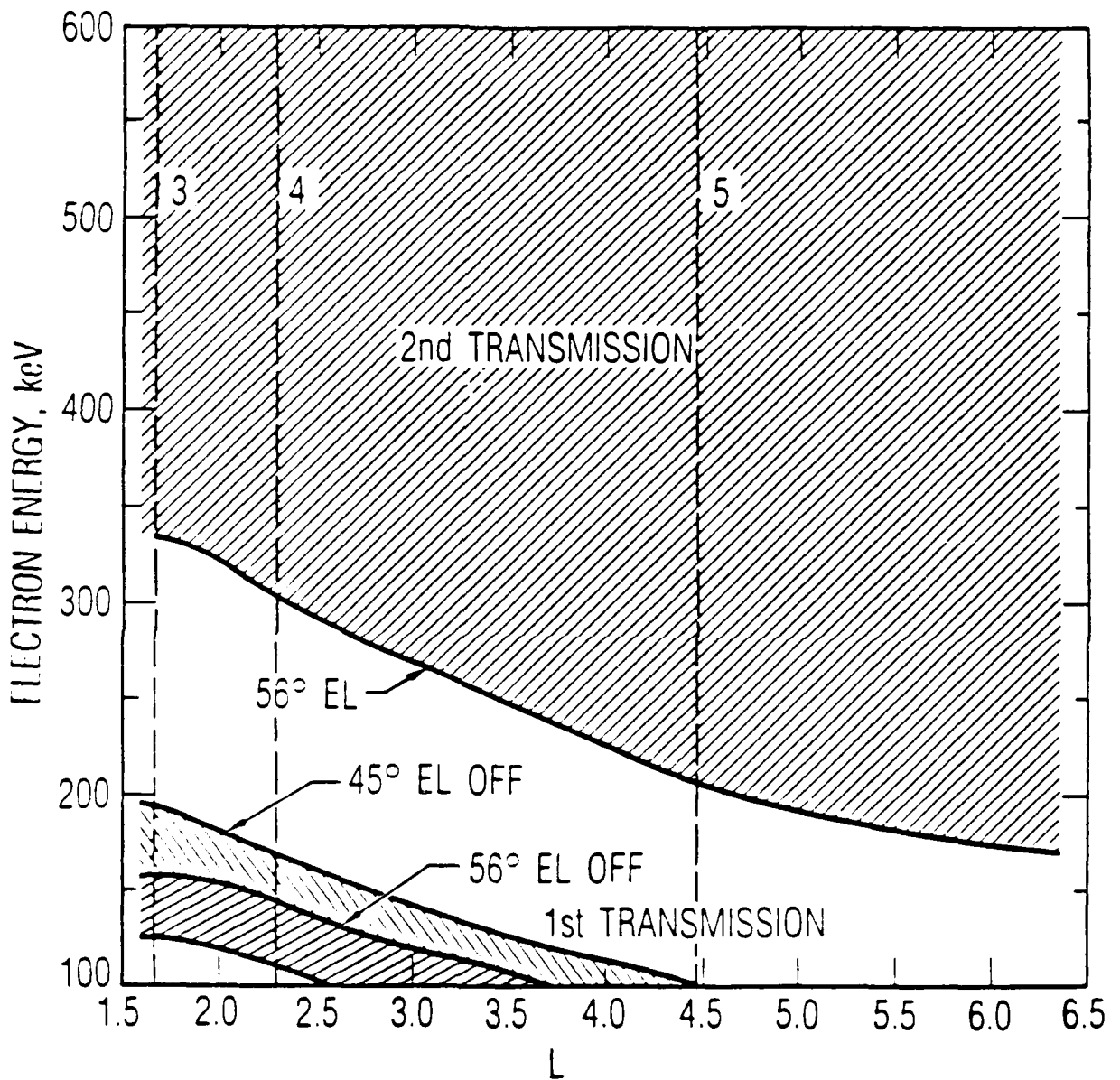
Figure 6. Diagram of the electron energies as a function of L which should be observable by the S3-3 satellite for the pass of Fig. 1 under the assumption that UMS precipitated electrons of all energies into the drift loss-cone during two specific transmission periods. Lines marked 45° and 56° indicate the longitude at which the precipitation is assumed to have occurred. Dashed lines marked 3-5 indicate the L-values of the peaks marked 3-5 in Fig. 1.

21

transmission and electrons with energies above about 335 keV precipitated by the second transmission should be observable at an L of 1.66. Additionally, electrons with energies between 155 keV and 195 keV precipitated at increasingly western longitudes to 45° should also be observable. Figure 1 shows that electrons are actually observed in the 108, 162, 235, and 433 keV channels. The 108 keV channel responds to particles with energies up to 118 kev and trails off to zero response at 121 keV. The 162 keV channel can respond to electrons with energies as low as 151 keV. Thus, electrons should be seen in the 108 and 162 keV channels, but with a very reduced intensity since the electron energies are near the limits of the response of the channels. This is what is seen. The 235 keV channel can respond to the 195 keV electrons precipitated by the first transmission, but again with very reduced intensity since the major response of that channel (80%) is above 200 keV. For the inner-zone event, the 235 keV channel traces back to 45° EL instead of 56° EL because electrons precipitated farther east which are in the major energy response of the channel have already drifted past the location of the satellite. The channel is even less sensitive to electrons with energies sufficiently low to have been precipitated east of 45° and still be intercepted by the satellite.

The second transmission might also have contributed to the response of the instrument at L=1.66. The 235 keV channel has a very small response at energies up to 430 keV, with perhaps 1% of its total response being above 365 keV. The very slight response in the 433 keV channel (which could respond only to electrons precipitated by the second transmission) and the lack of a response in the higher energy channels is undoubtedly due to the fact that significant numbers of electrons with energy above 400 keV are not precipitated in the inner zone by UMS [Vampola and Kuck, 1978]. On the basis of the transmitting schedule of UMS, electron drift times, and inner-zone precipitation energy spectra, electrons should be seen in the 108, 162, 235, and possibly the 433 keV channels. That is precisely what is observed. The drift-time analysis also properly explains the traceback to 45° EL for peak 3.

The slot precipitation analysis is similar. For this event, electrons were observable in all channels up to the 654 keV channel. Electrons precipitated by the first transmission should be observable in the 108 and 162 keV channels, while electrons above 300 keV from the second transmission should be seen in the other channels. The 235 keV channel has 20% of its response above 320 keV and was undoubtedly measuring electrons above 300 keV, although the measured intensity seems high for a channel whose major response is below this energy. The higher energy channels

22

were seeing particles of appropriately higher energy which were precipitated by the second transmission. The drift analysis based on the known transmission times and location again properly accounts for details of the particle observations. This analysis, together with the fact that UMS was currently precipitating inner-zone electrons, adds strong evidence to previous claims that ground-based VLF transmitters are responsible for significant precipitation in the slot [Vampola, 1977a; Vampola, 1987]. An important point to consider is that, unlike inner-zone VLF transmitter-induced precipitation, slot precipitation by ground-based VLF transmitters precipitates electrons with energies well above 400 keV.

Ground-based VLF transmitter precipitation of electrons from the inner zone is now generally acknowledged by the scientific community; slot precipitation produced by the same transmitters has received much less acceptance. Precipitation of outer zone electrons by these same transmitters has not been considered previously. If such a mechanism is operating, the implications of it to the morphology of the electron population of the magnetosphere, and our understanding thereof, are profound. Following the analyses used for the inner zone and slot observations, we can similarly analyze the outer zone precipitations seen in Fig. 1.

Figure 6 shows that even the lowest energy electrons from the first transmission would have drifted past the longitude of the satellite prior to the arrival of the satellite at the longitude of observation. Only electrons with energies above 210 keV precipitated by the second transmission would be observable by the satellite at the time and longitude of observation. Electrons were actually seen in the 235, 433, and 654 keV channels. A very important point is that no electrons were observed in the 108 and 162 keV channels. Electrostatic wave scattering [Koons et al, 1972] or magnetospheric hiss and chorus would not be energy selective and would, in fact, be expected to scatter low energy electrons more efficiently than high energy electrons. The high altitude measurements in the outer zone on the same orbit showed electrons with energies in the 108 and 162 keV channel range were present in significant numbers. In the drift loss cone, electrons are observed specifically in the 235, 433, and 654 keV channels not because only those energies are being precipitated, but because lower energy electrons from the first transmission had already drifted past the longitude of observation and those from the second transmission have not yet had time to drift to the longitude of observation.

We have, in this event, very significant precipitation of energetic electrons in the outer zone which is completely accounted for in every detail by using, as its source, precipitation over UMS while UMS was transmitting. Conversely, the energy spectrum of the precipitation is unlike that which would be produced by any other known source. The observation was obtained in close association with observations of precipitation by that same transmitter in the inner zone and in the slot. This and the agreement between the transmission schedule and the drift-rate analysis, we believe, unambiguously identifies this outer zone precipitation as being caused by UMS and establishes a previously unknown phenomenon: precipitation of energetic outer zone electrons by ground-based VLF transmitters. Additional support for the conclusion that UMS produces energetic electron precipitation in the outer zone can be gained from resonance calculations.

RESONANCE CALCULATIONS

In addition to establishing that resonance can occur between whistler-mode VLF waves with the frequency of UMS and gyrating electrons of the energy observed in this study, another rationale for performing resonance calculations is the determination of the probable location on the field line for the gyroresonant interaction. A number of investigations of wave-particle interactions in the magnetosphere have been made previously with various assumptions. For instance, Helliwell et al [1975] assumed interactions with ducted waves in the equatorial region because such conditions allowed a more tractable calculation. Inan et al [1978] simulated interactions between coherent waves and low energy electrons and found that the interaction is linear when the wave intensity is low compared to the transverse energy of the particle (3 pT for 1 keV electrons at 10° pitch-angle) or for interactions away from the equator where the inhomogeneity of the medium dominates. Koons et al [1981] utilized wave-tracing of non-ducted wave propagation to an inner-zone interaction region near the equator in comparisons with L-dependent energetic electron precipitations. Vampola [1977a] hypothesized wave-particle interactions in the slot region much lower on the field line but did not present detailed calculations.

Results of calculations have been consistent with observations. Koons et al [1981] calculated that a field intensity of 3 pT was sufficient to produce the scattering they observed, while the calculation of electron interaction with coherent waves reported by Inan et al [1983] indicated that detectable electron scattering should be accomplished with as little as 1 pT. They considered low energy, a few keV, electrons and assumed ducting. Inan et al [1977] reported in-situ measurements near the equator of 0.1 to 0.3 pT levels from the Siple transmitter before magnetospheric amplification and also reported observation of an amplified wave prior to its first passage through the equatorial region, indicating that wave-particle interactions could occur well away from the equator.

Because the ionosphere is a magnetized plasma, its properties are anisotropic for radio waves reflecting off of it or propagating through it. Furthermore, it is generally highly attenuating. As a result, realistic calculations of wave propagation have not been made in analytic form. Instead, ray-tracing techniques are used. The advantage of ray-tracing is that one can describe the propagation medium in either continuous or discrete form and make relatively good predictions of the resultant wave propagation vector and amplitude without resorting to ducts. Con-

jugate studies have shown wave propagation between mid-latitude conjugate points. Ducting is usually given as the explanation. Direct propagation requires that an otherwise reflecting iono- sphere be sufficiently transparent to waves for significant en- ergy to leak through to the duct.

The geometry of the calculation of resonance between whistler-mode waves and energetic electrons is as follows: VLF waves from a ground-based transmitter in the northern hemisphere, propagating upward and southward in an unducted mode, interact with energetic electrons travelling northward and downward along the local magnetic guiding center. Some of the electrons interact gyroresonantly with the waves, giving up some of their transverse energy. In the potential well of the wave, some transverse energy is also converted to parallel energy [Inan et al, 1983]. The wave is amplified and the local pitch angle of the particle is re- duced. If sufficient energy transfer occurs or if sufficient en- ergy is lost, the pitch angle may be reduced sufficiently to lower the particle's mirror altitude to below the atmospheric cutoff (100 km). Particles with lowered pitch angles which escape being lost into the atmosphere at the longitude of the transmit- ter drift eastward where they may be observed by the S3-3 instru- ment and are ultimately lost into the atmosphere at a longitude where the earth's field at 100 km or below is weaker than the mirror B for the particle.

The resonance condition for an unducted whistler-mode wave of frequency ω and wave normal θ interacting with a relativistic electron with a local pitch angle α is given by

$$\omega(1 - \beta\mu\cos\theta\cos\alpha) = m\Omega_c(1 - \beta^2)^{1/2}$$

where $\beta = v/c$, v is the electron velocity, Ω_o is the cold elec- tron gyrofrequency, m is the order of the resonance, and μ is the index of refraction, given by

$$\mu = \{1 + \omega_p^2/[\omega(\Omega_c\cos\theta - \omega)]\}^{1/2}$$

where $\omega_p{}^2$ is the plasma frequency, squared, and is given by

$$\omega_p{}^2 = 4\pi q_e{}^2 N_e [(1/m_e) + (1/m_p)]$$

where N_e is the local plasma density, q_e is the electron charge, and m_i is the rest mass of the electrons/ions making up the plasma. In a realistic plasmaspheric model, a combination of protons and singly-ionized oxygen ions is usually used and an appropriately weighted mass is used for computing the plasma frequency.

Figure 7 shows the resonant energy as a function of altitude for first order resonance with unducted waves for the three regions of precipitation discussed in this study. The frequency was selected to correspond to that of UMS; the base density for a diffusive equilibrium model of the plasmasphere was selected to give a best fit to the inner-zone precipitation data; and, the H^+/O^+ ratio was set at a nominal 90%/10% at a temperature of 1600 °K (following Koons et al [1981]). The L values selected are those which are representative of the center of the precipitation peaks in the 235 keV channel. The index of refraction and wave normal angle were determined using a wave-tracing procedure based on the work of Burtis [1973] as modified by Edgar [1976] and Thomson [1976]. The Thomson modification is a provision for varying the latitude at which the light ion and heavy ion densities are equal. The modification, called the Transition Level Gradient (TLG) model, provided a better fit to the data of ISIS II than the original Burtis codes as modified by Edgar. The base density for a diffusive-equilibrium model of the ionosphere/plasmasphere was selected on the basis of a best fit to the 235 keV channel data at L=1.66. The selected equatorial pitch angle of the electron is that which just permits a particle to survive drift through the South Atlantic Anomaly. This value was selected on the basis that it requires the minimal change in pitch angle (and energy loss) to precipitate it into the bounce or drift loss cone.

The resonance calculation is not completely consistent internally, since the ray-tracing codes used a dipole field model while the resonance calculation followed the field line using the same field model as was used in the drift-rate and longitude-of-origin studies: DGRF 1975 [IAGA, 1981], Epoch 1976. The ray tracing procedure assumed that waves were injected vertically, giving an initial wave-normal angle equal to the local dip-angle of the field line. The waves did not follow the field line, but a series of traces at slightly different latitudes (plus or minus a few degrees around the latitude of the transmitter) were used to determine the wave-normal angle and index of refraction at a number
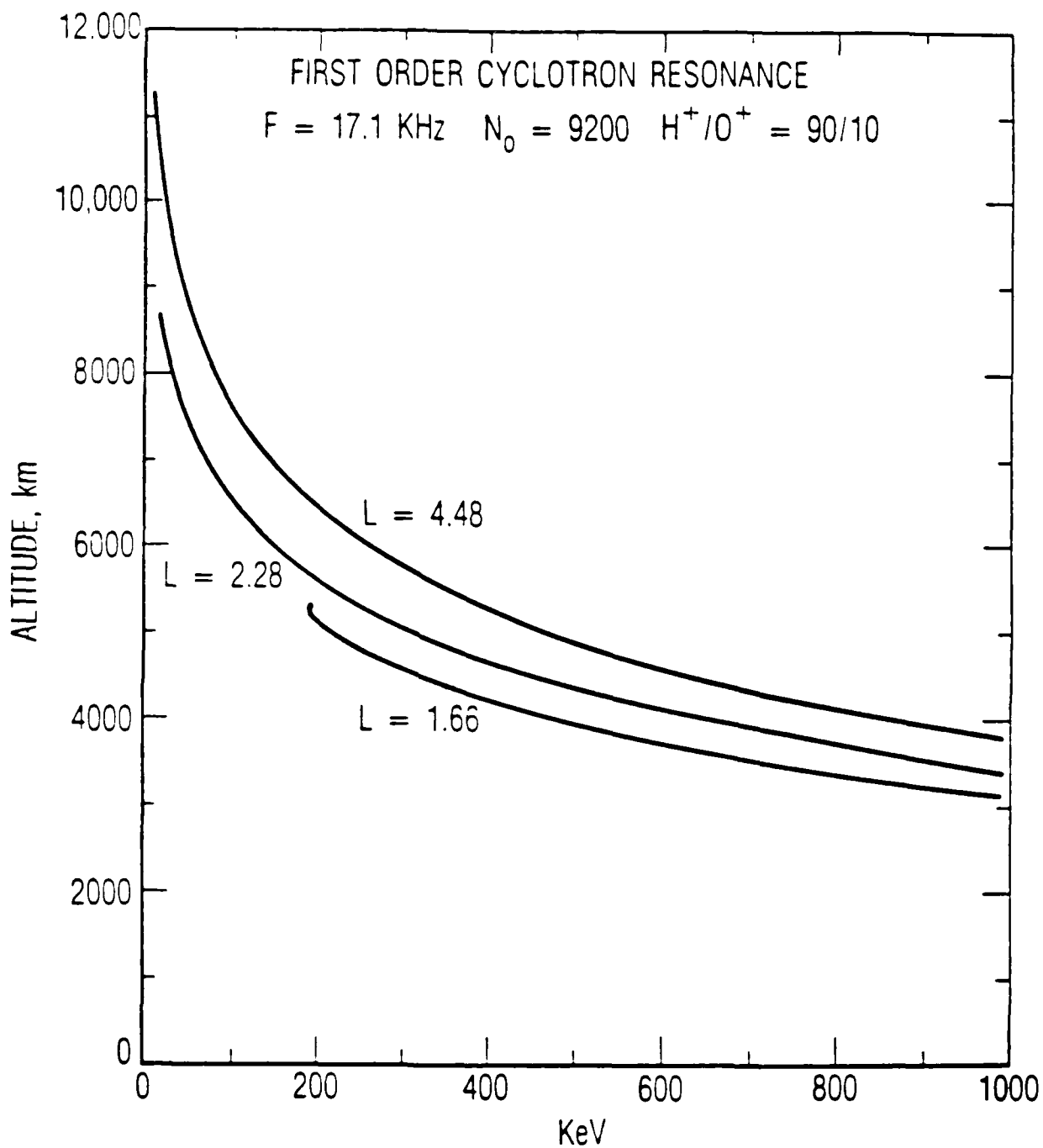
Figure 7. Calculations of resonance between energetic electrons and 17.1 kHz waves. Resonance regions are shown which compare with the data of Figs. 3, 4, and 5. The L=1.66 resonance for 195 KeV electrons is at the equator. The other resonance locations are well off the equator at altitudes of 5000 to 6000 km.

of points along the field line. In the resonance calculation, interpolation was then used to determine the local wave-normal and local index of refraction.

Figure 7 shows that first order resonance conditions for electrons of the energy (~300 KeV) and L-value (2.28) of Fig. 4 are obtained in the vicinity of 5000 km, well away from the equator. For resonance to occur near the equator with the particles observed by the S3-3 at this L-value, transmitter frequencies below 2000 Hz would be required, well below operational VLF transmitter frequencies. For resonance to occur at the equator with the appropriate frequency (UMS) and electron energy, the initial pitch angle would have to be large (which leads to an unrealistically large initial energy and energy loss). For L=4.48, Fig. 7 shows that resonance with the observed energies can occur in the vicinity of 6000 km.

The equatorial region is usually selected as the location of a possible wave-particle interaction region on the basis that the resonance conditions remain relatively constant for a greater distance along the field line there than elsewhere, since B (which determines the local cold electron gyrofrequency) and N_e are relatively constant there and α and θ change more slowly there. The L=1.66 curve in Fig. 7 indicates that for a small region around the equator, the resonant energy decreases slightly as the particle goes away from the equator, enabling the particle to stay in resonance as it loses energy. Evaluation of precipitation events in the inner zone (Koons et al [1981]) indicated that the resonance region was near-equatorial. This is also true of low energy electron precipitation in the lower portion of the slot [Imhof et al, 1983] (which may have been just a continuation of the inner-zone precipitation, extending to very low energy and therefore up to slot altitudes). But, for energetic electron precipitation in the central portion of the slot, E>200 keV, L~2.3, resonance conditions can be met at the equator only for a high order resonance or unrealistic conditions. However, examination of the resonance conditions shows that an electron going down the field line may continue in resonance as long as the rate at which it is losing energy (which decreases α and β) just balances the changes in θ, which decreases, and μ and Ω_o, both of which increase at lower position on the field line. Since the potential well of the wave may also be converting transverse energy to parallel energy elastically, the picture can become quite complicated. A thorough discussion of this point is beyond the scope of this paper, but the observation of a Siple Station VLF transmission being amplified prior to its first passage through the equatorial region [Inan et al, 1977] can be taken as evidence that off-equatorial wave-particle resonant interactions do occur.

DISCUSSION and SUMMARY

Drift-rate analysis of electrons observed in the drift loss cone, coupled with the operating sequence of the VLF transmitter UMS, explains the detailed electron observations as a function of energy for several different L-shells. Additionally, the pitch-angle distributions which are observed are consistent with those that would be produced if the electrons had been precipitated in the vicinity of UMS. The combination of pitch-angle and energy observations are consistent in every detail with a scenario in which UMS precipitated electrons over a wide energy range in several different L-shells, including the outer zone.

A number of questions remain: a) Why has precipitation of outer-zone electrons by VLF transmitters not been observed previously? b) Why does the precipitation at a given energy occur at discrete L-values instead of being a continuum over the slot and outer zone? Is this related to the plasmaspheric structure? c) How important is the precipitation of electrons by VLF stations in the outer zone and, more importantly, in the morphology of the magnetospheric particle population? Is it the primary controlling factor?

The first of these questions may have the simplest answer: Outer zone precipitation of electrons by ground-based VLF transmitters may not have been observed previously because almost no one has looked for it. The SEEP experiment (Imhof et al [1983]) attempted to observe outer zone precipitation and was unsuccessful. (The reason for this lack of success might be because NAA does not precipitate outer zone electrons as does UMS or it might be due to a lack of sufficient intensity in precipitated outer zone electrons during that campaign to be observed by the SEEP experiment. In the S3-3 data set, only 7% of the orbits had outer zone precipitations which were thought to be due to VLF transmitters.) In the outer zone, a number of other processes precipitate electrons. During magnetic storms, intense precipitation at all energies is observed at high latitudes. During minor disturbances, the outer edge of the outer zone, as observed by low altitude satellites, moves in and out significantly due to relatively low altitude processes [Vampola, 1977b]. In order to establish that a given precipitation event is due to a specific VLF transmitter, a lengthy pitch-angle distribution analysis must be performed which is not easily automated because it must identify the structure as being in the drift loss cone, as having a distribution that is narrower than the local loss cone, and as

31

having a distribution that was not determined by the South Atlantic Anomaly (or a similar magnetic structure in the vicinity of 180° EL). Most electron spectrometers flown on satellites do not obtain complete pitch angle distributions. For measurements made at higher altitudes in the stable trapping region, high angular definition is required in order to utilize the trace-back technique. Even with an appropriate data set, without the suspicion that a given precipitation event had as its source a VLF transmission, the extensive analysis required to establish it as such would not be done. The present analysis is the result of a survey of data looking for slot precipitation events due to UMS. In the course of the survey, it became evident that outer zone precipitation in the few-hundred keV range was frequently related to the presence or absence of an energy-dependent slot peak. Furthermore, the outer zone peak, while not appearing to be L-dependent, exhibited strange energy behavior (occasionally low energy electrons were not observed and in some events the 433 keV channel had much higher fluxes than the 235 keV channel).

The second question is more difficult to answer. The ray-tracing "exercises" were instructive and offer several possible answers. First, under some conditions of injection latitude, injection angle, and plasmaspheric configuration, the waves follow the field line quite closely for a significant distance and provide a large path-length and interaction time with coherent conditions and very slow change in resonant energy which may enhance scattering for low signal levels. Perhaps waves must be injected with specific latitude and plasmaspheric conditions to produce precipitation. Then injection of waves at various latitudes would be responsible for the several L-regions of precipitation. A second observation was that waves injected at several latitudes may all pass through the same region of the magnetosphere, a "focusing" effect, which could provide constructive interference to enhance the wave-field levels at those points. Perhaps precipitation occurs on discrete L-shells due to discrete regions of constructive interference. The loci at which the several ray paths intersect are at high latitude well away from the equator. Another possibility is that waves amplified by interacting with electrons at low L (e.g., inner zone, equator) are later reflected at high latitude and travel back upward toward the equator to again interact with electrons on a higher L-shell (but not necessarily near the equator). These waves could be again amplified, again reflected, and again interact with electrons on a yet higher L-shell. Assuming sufficient reflection (the product of amplification and reflectivity being greater than unity), the interaction could be between upward-going waves and downward-going particles, as assumed for the earlier discussion, or with upward-travelling particles and downward-going waves, in either hemi-

32

sphere. Thus the pattern of precipitation in L could be due to the specifics of magnetospheric wave propagation from a single injection point or multiple injection points. Inhomogeneities in the ionosphere and plasmasphere could play a crucial role. Finally, it may be possible that electrons are indeed precipitated throughout the magnetosphere above L=2 but their appearance in the drift loss cone is dependent on the intensity at higher altitudes. Further investigations along this line are planned but the present ray-tracing codes will have to be integrated with real magnetic field models and in-situ measurements of electron density profiles in order to provide reliable numerical results.

The last question, *how important is the precipitation of outer-zone electrons by VLF stations,* is probably answerable by a number of means: 1. Turn off all VLF stations for a few months and observe the behavior of the energetic electrons in the magnetosphere. (Use only satellites for navigation and communication during that period.) This method has the disadvantage that if the VLF transmitters are crucial in determining the structure of the electron belts, the inner zone could become extremely hazardous to satellites through a build-up of relativistic electrons diffusing inward from the outer zone. 2. Do an inventory of electrons in the drift and bounce loss cones to determine where they left the stable trapping region. (Previous studies have tended to look for the longitude at which the drifting electrons would enter the atmosphere, since that is a much more easily determined parameter.) This is a large undertaking, but would not require the cooperation of the various nations operating high-powered VLF transmitters and would not be potentially hazardous. 3. Make simultaneous measurements of high altitude and drift shell electron fluxes during a magnetically quiet period and attempt to determine the lifetime of electrons due to removal by VLF transmission precipitation and compare those lifetimes to radial diffusion coefficients determined from the same data set. This study would require a dense data set, probably obtained simultaneously by several satellites.

REFERENCES

Burtis, W. J., _User's guide to the Stanford VLF raytracing program_, Radioscience Lab., Stanford University, 1973

Edgar, B. C., The theory of VLF Doppler signatures and their relation to magnetospheric density structure, J. Geophys. Res., 81, 3327, 1976

Helliwell, R. A., J. P. Katsufrakis, T. F. Bell, and R. Raghuram, VLF line radiation in the earth's magnetosphere and its association with power system radiation, J. Geophys. Res., 80, 4249, 1975

IAGA Division 1 Working Group 1, International Geomagnetic Reference Field 1980, IAGA News No. 20, Dec. 1981, p. 100 (also EOS, June 17, 1986, p. 523)

Imhof, W. L., R. R. Anderson, J. B. Reagan, and E. E. Gaines, The significance of vlf transmitters in the precipitation of inner belt electrons, J. Geophys. Res., 86, 11225, 1981

Imhof, W. L., J. B. Reagan, H. D. Voss, E. E. Gaines, D. W. Datlowe, J. Mobilia, R. A. Helliwell, U. S. Inan, J. Katsufrakis, and R. G. Joiner, Direct observation of radiation belt electrons precipitated by the controlled injection of VLF signals from a ground-based transmitter, Geophys. Res. Lett., 10, 361, 1983

Inan, U. S., T. F. Bell, D. L. Carpenter, and R. R. Anderson, Explorer 45 and IMP 6 observations in the magnetosphere of injected waves from the Siple Station VLF transmitter, J. Geophys. Res., 82, 1177, 1977

Inan, U. S., T. F. Bell, and R. A. Helliwell, Nonlinear pitch angle scattering of energetic electrons by coherent VLF waves in the magnetosphere, J. Geophys. Res., 83, 3235, 1978

Inan, U. S., T. F. Bell, and H. C. Chang, Particle precipitation induced by short-duration VLF waves in the magnetosphere, J. Geophys. Res., 87, 6243, 1983

Koons, H. C., A. L. Vampola and D.A. McPherson, Strong pitch-angle scattering of energetic electrons in the presence of electrostatic waves above the ionospheric trough region, J. Geophys. Res., 77, 1771, 1972

Koons, H. C., B. C. Edgar, and A. L. Vampola, Precipitation of inner-zone electrons by whistler mode waves from the VLF transmitters UMS and NWC, J. Geophys. Res., 86, 640, 1981

Luhmann, J. G. and A. L. Vampola, Effects of localized sources on quiet time plasmasphere electron precipitation, J. Geophys. Res., 82, 2671, 1977

Schulz, M. and L. J. Lanzerotti, Particle Diffusion in the Radiation Belts, p. 67, Springer, New York, 1974

Thomson, R. J., VLF Propagation in the Magnetosphere, Ph. D. Thesis, University of Otago, 1976

Vampola, A. L., VLF transmission-induced slot electron precipitation, Geophys. Res. Lett., 4, 569, 1977a

Vampola, A. L., The effect of strong pitch-angle scattering on the location of the outer zone electron boundary as observed by low-altitude satellites, J. Geophys. Res., 82, 2289, 1977b

Vampola, A. L., Observations of VLF transmitter-induced depletions of inner zone electrons, Geophys. Res. Lett., 10, 619, 1983

Vampola, A. L., Electron Precipitation in the Vicinity of a VLF transmitter, J. Geophys. Res., 92, 4525, 1987

Vampola, A. L. and G. A. Kuck, Induced precipitation of inner zone electrons: 1. Observations, J. Geophys. Res., 83, 2543, 1978

Vampola, A. L. and D. J. Gorney, Electron energy deposition in the middle atmosphere, J. Geophys. Res., 88, 6267, 1983

Watt, A. D., VLF Radio Engineering, Pergamon Press, Oxford, 1967

The Aerospace Corporation functions as an "architect-engineer" for national security projects, specializing in advanced military space systems. Providing research support, the corporation's Laboratory Operations conducts experimental and theoretical investigations that focus on the application of scientific and technical advances to such systems. Vital to the success of these investigations is the technical staff's wide-ranging expertise and its ability to stay current with new developments. This expertise is enhanced by a research program aimed at dealing with the many problems associated with rapidly evolving space systems. Contributing their capabilities to the research effort are these individual laboratories:

Aerophysics Laboratory: Launch vehicle and reentry fluid mechanics, heat transfer and flight dynamics; chemical and electric propulsion, propellant chemistry, chemical dynamics, environmental chemistry, trace detection; spacecraft structural mechanics, contamination, thermal and structural control, high temperature thermomechanics, gas kinetics and radiation; cw and pulsed chemical and excimer laser development including chemical kinetics, spectroscopy, optical resonators, beam control, atmospheric propagation, laser effects and countermeasures.

Chemistry and Physics Laboratory: Atmospheric chemical reactions, atmospheric optics, light scattering, state-specific chemical reactions and radiative signatures of missile plumes, sensor out-of-field-of-view rejection, applied laser spectroscopy, laser chemistry, laser optoelectronics, solar cell physics, battery electrochemistry, space vacuum and radiation effects on materials, lubrication and surface phenomena, thermionic emission, photo-sensitive materials and detectors, atomic frequency standards, and environmental chemistry.

Computer Science Laboratory: Program verification, program translation, performance-sensitive system design, distributed architectures for spaceborne computers, fault-tolerant computer systems, artificial intelligence, micro-electronics applications, communication protocols, and computer security.

Electronics Research Laboratory: Microelectronics, solid-state device physics, compound semiconductors, radiation hardening; electro-optics, quantum electronics, solid-state lasers, optical propagation and communications; microwave semiconductor devices, microwave/millimeter wave measurements, diagnostics and radiometry, microwave/millimeter wave thermionic devices; atomic time and frequency standards; antennas, rf systems, electromagnetic propagation phenomena, space communication systems.

Materials Sciences Laboratory: Development of new materials: metals, alloys, ceramics, polymers and their composites, and new forms of carbon; non-destructive evaluation, component failure analysis and reliability; fracture mechanics and stress corrosion; analysis and evaluation of materials at cryogenic and elevated temperatures as well as in space and enemy-induced environments.

Space Sciences Laboratory: Magnetospheric, auroral and cosmic ray physics, wave-particle interactions, magnetospheric plasma waves; atmospheric and ionospheric physics, density and composition of the upper atmosphere, remote sensing using atmospheric radiation; solar physics, infrared astronomy, infrared signature analysis; effects of solar activity, magnetic storms and nuclear explosions on the earth's atmosphere, ionosphere and magnetosphere; effects of electromagnetic and particulate radiations on space systems; space instrumentation.

. . .

END

DATE FILMED

FILMED

6-88

DTIC